Proc. Natl. Acad. Sci. USA
Vol. 91, pp. 3049–3053, April 1994
Developmental Biology

Vertical versus planar neural induction in *Rana pipiens* embryos

(gastrulation/neural induction/amphibian)

JEAN-PIERRE SAINT-JEANNET* AND IGOR B. DAWID†

Laboratory of Molecular Genetics, National Institute of Child Health and Human Development, National Institutes of Health, Bethesda, MD 20892

Contributed by Igor B. Dawid, December 20, 1993

ABSTRACT **The neural plate in the amphibian embryo is induced in the ectoderm by signals from the dorsal mesoderm. In the extensively studied species *Xenopus laevis*, such signals are believed to proceed along two alternate pathways, defined as vertical and planar induction. We have studied the relative importance of these pathways in *Rana pipiens*. In the embryo of this frog, dorsal mesoderm involution can be diverted from its normal course by injection of peptides that inhibit interaction of fibronectin with its receptor. In such embryos, dorsal mesoderm failed to migrate across the blastocoel roof but moved bilaterally along the equator, leading to the formation of two notochords. Neural tissue differentiation occurred in close association with each notochord, but no neural tissue formed along the dorsal midline as might have been predicted by a predominantly planar induction model. While in *X. laevis* planar induction has been reported to be a major pathway in neuralizing the ectoderm, the results presented here indicate that vertical induction predominates in initiating neural development in *R. pipiens* embryos.**

Development of the vertebrate nervous system begins with the induction of the neural plate from uncommitted ectoderm in response to signals from the dorsal mesoderm. Classical grafting experiments in newts (1–5) led to the view that induction and patterning along the anteroposterior (A–P) axis of the nervous system result from vertical signaling from the involuting dorsal mesoderm to the overlying ectoderm. However, recent results in *Xenopus laevis* indicate that neural differentiation and patterning can also be initiated by planar signals that spread from the dorsal mesoderm through the plane of the ectoderm (6–10). This conclusion is based on observations of exogastrulae (11–14) and Keller explants (14–17), in which vertical contact is believed to be absent. In the ectoderm of exogastrulae and Keller explants, several pan-neural genes including *NCAM* and *NF3* (11, 13–15), and the position-specific neural genes *Xhox3, engrailed, Krox-20, XlHbox1 (Hox C6), XlHbox6 (Hox B9), Xdll-3*, and *XASH-3* (12, 13, 15–17) were found to be expressed at normal levels and in a correct A–P pattern; however, other neural genes such as *XIF3, XFKH1/Pintallavis* and *Xlim1* failed to be induced in these preparations (18–20, 49). Dorsal mesoderm in exogastrulae evaginates away from the ectoderm by complex cell movements that remain poorly studied, and vertical contacts cannot be fully excluded. Keller explants (21) have the advantage that the absence of mesoderm ingression into the ectoderm has been demonstrated by lineage labeling (22, 23), but early molecular markers have not been used to identify mesodermal cells and their migration behavior in such explants.

A useful preparation for the study of mesoderm–ectoderm interactions was suggested by the work of Boucaut, Johnson, and their colleagues (reviewed in refs. 24 and 25). In the urodele *Pleurodeles waltl* and the frog *Rana pipiens*, dorsal mesoderm involutes along the midline of the ectoderm by migration on a fibronectin-rich extracellular matrix that covers the blastocoel roof (24, 26). Injection of peptides that carry the RGD (Arg-Gly-Asp) recognition motif of the fibronectin molecule for its receptor, or of antibodies that block this interaction, into the blastocoel of pregastrula embryos prevents migration of the mesoderm across the blastocoel roof of these amphibians (27–29). This is not the case in *X. laevis* embryos in which substrate-independent convergence and extension movements within the mesoderm dominate gastrulation (30, 31).

We have used GRGDS peptide-injected *R. pipiens* embryos to analyze ectoderm–mesoderm interactions during neural development. The properties of such embryos allow a clear prediction: since a dorsal blastopore lip forms but the mesoderm does not involute (ref. 29; *Results*), a planar signal is expected to emanate from the region of the dorsal lip in the same way in injected and control embryos. If such a signal is sufficient, in the context of the whole embryo, to induce neural development, at least some neural differentiation should arise along the dorsal midline of the peptide-injected embryos. In this paper we report the results of a test of this prediction.

MATERIALS AND METHODS

Embryos. *R. pipiens* were obtained during the fall from C. D. Sullivan (Nashville, TN) and Hazen (Alburg, VT) and maintained at 4°C until use. Females were induced to ovulate as described (32, 33). One hour after fertilization eggs were dejellied in a large volume of 2% cysteine (pH 7.7). Embryos were reared in 20% Steinberg's solution (34) and staged according to Shumway (35).

Microinjection of Peptides. The inhibitor peptide GRGDS (Gly-Arg-Gly-Asp-Ser) and the related peptide GRGES (Gly-Arg-Gly-Glu-Ser) were purchased from Sigma and Peninsula Laboratories, respectively. Peptides were dissolved in 20% Steinberg's solution by vigorous agitation. For injections (28, 29), embryos at the late blastula stage (stage 9) were placed in the wells of a Terasaki dish in 20% Steinberg's solution plus 5% Ficoll (Sigma). Glass capillaries were used with a tip diameter of 20 μm. About 200 nl of blastocoel fluid was aspirated and replaced by the same volume of peptide solution. One hour after injection embryos were transfered to 20% Steinberg's solution and cultured at 18°C.

Antibodies. 4d (36, 37), LINC (38), and 12/101 (39) hybridoma supernatants were obtained from the Developmental Studies Hybridoma Bank maintained by the Department of Biology, University of Iowa, under Contract NO1-HD-2-

The publication costs of this article were defrayed in part by page charge payment. This article must therefore be hereby marked "*advertisement*" in accordance with 18 U.S.C. §1734 solely to indicate this fact.

Abbreviations: A–P, anteroposterior; CNS, central nervous system; TRLDX, Texas Red lysine dextran; FLDX, fluorescein lysine dextran; AMCA, aminomethylcoumarin acetate.

*Permanent address: Centre de Biologie du Dévelopement, Centre National de la Recherche Scientifique-Unité Mixte de Recherche 9925, Université Paul Sabatier, 118 route de Narbonne, 31062 Toulouse Cedex, France.
†To whom reprint requests should be addressed.

3144 from National Institute of Child Health and Human Development. Tor 70 (40) ascites fluid was a gift of P. Kushner and R. Harland (Berkeley, CA). Secondary antibodies conjugated to peroxidase and alkaline phosphatase were from Amersham and Boehringer Mannheim, respectively.

Immunocytochemistry. Whole-mount immunostaining followed a previously published protocol, where abbreviations for reagents and solutions are listed (41). Briefly, embryos were fixed in MEMFA for 1 hr and then bleached in methanol/hydrogen peroxide for 8 days (time required for these highly pigmented embryos to turn yellow). Embryos were rehydrated in PBS and incubated for 1 hr in PBT plus 10% inactivated sheep serum, incubated successively with primary and secondary antibodies overnight at 4°C, washed extensively, and stained by enzymatic reaction. The reaction was stopped in methanol and the embryos were cleared in BA/BB. For double staining, the two reactions were carried out consecutively.

Lineage Tracing. Blastomere nomenclature at the 32-cell stage was according to Nakamura and Kishiyama (42). In *R. pipiens* the grey crescent, which defines the prospective dorsal side, can easily be identified at least until the late blastula stage. Two blastomeres and their counterparts across the midline were injected with 2–5 nl of either Texas Red lysine dextran (TRLDX) or fluorescein lysine dextran (FLDX) (both M_r 10,000, Molecular Probes) at 10 mg/ml in water. When embryos reached stage 9, a subset was injected with GRGDS peptide. At stage 21 (early tadpole), embryos were fixed in methanol at −80°C and transfered gradually to room temperature. Embryos were then immersed in xylene and embedded in Paraplast, and 10-μm sections were collected on glass slides. Sections were deparaffinized, rehydrated, incubated with a mix (1:1) of 4d and LINC antibodies, and stained by successive incubation with anti-mouse biotinylated IgG (Amersham) and streptavidin conjugated to aminomethylcoumarin acetate (AMCA, The Jackson Laboratory), allowing identification of neural cells by blue color. Sections were then mounted in glycerol and observed with a Zeiss Axiophot fluorescence microscope using a Chroma dual-band filter set for fluorescein and Texas Red.

RESULTS

Inhibition of Gastrulation by Peptide Injection. Different concentrations of peptides were tested ranging from 5 to 50 mg/ml (not shown), and the concentration of 50 mg/ml was chosen for these experiments as the maximally effective but essentially nontoxic dose, allowing 92% survival. At the early gastrula stage (stage 10), GRGDS-injected *R. pipiens* embryos formed an apparently normal dorsal blastopore lip (Fig. 1 *A* and *B*), but by late gastrula (stage 12), a majority (69%, n = 247) displayed incomplete blastopore closure (Fig. 1 *C* and *D*). As controls reached tailbud stages (Fig. 1*E*), GRGDS-injected embryos elongated, with a large mass of endomesoderm protruding from the open blastopore (Fig. 1*F*). Embryos with this phenotype (Fig. 1*F*) will hereafter be referred to as GRDGS embryos. Injections of the related peptide, GRGES, at the same concentration generated a similar phenotype in only 23% of the embryos analyzed (n = 130). It has been reported that GRGES has a much lower but discernable inhibitory effect on the binding of cells to fibronectin (43).

Differentiation of Axial Mesoderm and Neural Tissue in GRGDS Embryos. We used monoclonal antibodies specific for skeletal muscle (12/101), notochord (Tor 70), and neural tissue (4d, anti-NCAM, and LINC) to characterize GRGDS embryos by whole-mount immunostaining. In normal embryos, 12/101 stains the somites (Fig. 2*A*), Tor 70 stains the notochord (Fig. 2*D*), and anti-NCAM (Fig. 2*G*) (as well as

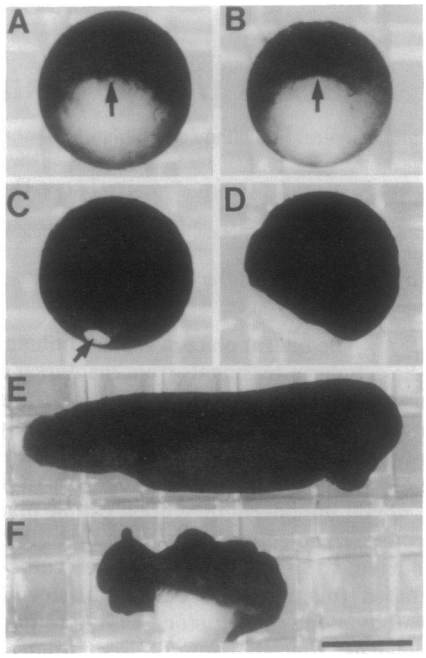

FIG. 1. Development of embryos injected at the blastula stage with 200 nl of GRGDS peptide at 50 mg/ml. At the early gastrula stage both control (*A*) and injected embryos (*B*) display an apparently normal blastopore lip (arrow) as viewed from the vegetal pole. At late gastrula, blastopore closure in the control embryo (*C*) is almost complete (arrow), but the injected embryo (*D*) shows a large yolk plug. By stage 20 [control at tailbud stage (*E*)], the endomesoderm of the injected embryo (*F*) protrudes from the blastopore that remains largely open. In *E* and *F*, anterior is to the right and dorsal is up. (Bar = 1 mm.)

LINC, not shown) stains the CNS. GRGDS embryos at equivalent stage 18 (Fig. 2 *B*, *E*, and *H*) and stage 20 (Fig. 2 *C*, *F*, and *I*) were stained with these four antibodies. In all embryos examined (n = 26), two parallel blocks of somites were seen dorsolaterally (Fig. 2 *B* and *C*); muscle differentiation and histogenesis were not grossly distorted in these embryos as suggested by the segmented pattern of the somites (Fig. 2*K*). In a large majority of these embryos (93%, n = 35) the two pairs of somites were associated with two independent notochords located bilaterally in an equatorial position (Fig. 2 *E* and *F*). Thus, GRGDS embryos had formed two axes that were positioned laterally.

Staining with 4d-NCAM or LINC antibodies showed bilateral expression of these neural markers in two extended structures of apparent neural tissue in 83% (n = 41) of GRGDS embryos (Fig. 2 *H–L*). GRGDS embryos doubly stained with Tor 70 and LINC or 4d-NCAM antibodies revealed that the LINC- or NCAM-expressing cells were always closely associated with each laterally positioned notochord (Fig. 2*L*); no NCAM- or LINC-positive cells were ever observed along the dorsal midline of the ectoderm. The putative neural tissue in GRGDS embryos formed a tube-like structure, displaying segmentation that may reflect the arrangement of spinal nerves (Fig. 2 *J* and *L*), but showing no indication of anterior patterning to form anything resembling a brain. However, suckers, which are ectodermal structures requiring induction for their formation, developed at the anterior end of 87% of the GRGDS embryos analyzed (n = 24, not shown). The cement gland of *X. laevis*, the homolog of the suckers, can be induced in the ectoderm by vertical contact with the dorsal mesoderm (44) and by planar signaling in exogastrulae (13) and Keller explants (16).

Lineage Derivation of the Notochord and Neural Tissues in GRDGS Embryos. Do the same cells that generate the dorsal axis in normal embryos contribute to the two axes of GRGDS

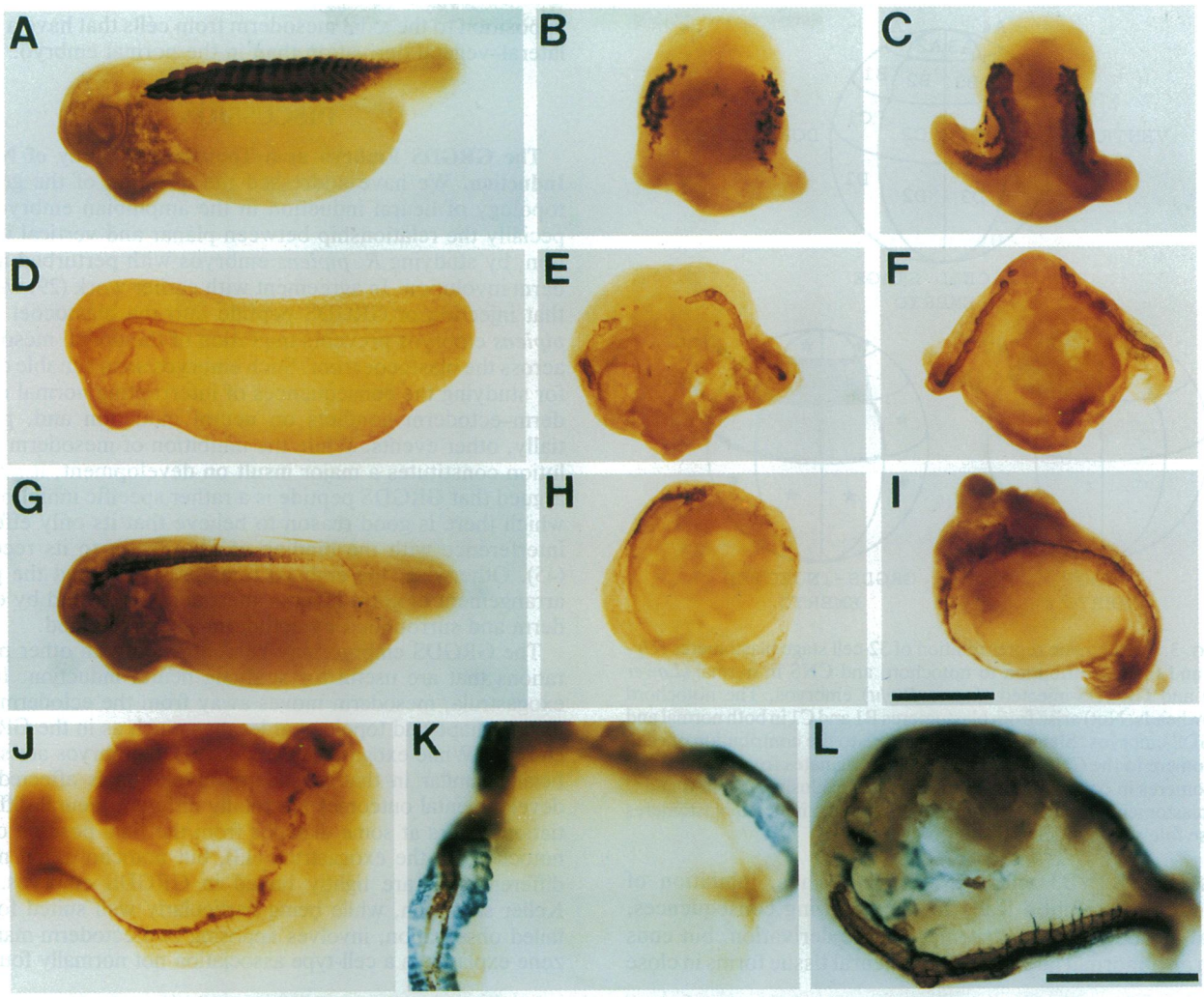

FIG. 2. Expression of differentiation markers visualized by whole-mount immunostaining in intact and GRGDS embryos. Control embryos at stage 18 (*A*, *D*, and *G*); GRGDS embryos at equivalent stage 18 (*B*, *E*, and *H*), stage 20 (*C*, *F*, *I*, and *J*), and stage 21 (*K* and *L*). Muscle-specific 12/101 monoclonal antibody (39) stains somites in control (*A*) and GRGDS embryos (*B* and *C*); note two sets of somites in *B* and *C*. Tor 70 monoclonal antibody specifically stains the notochord in *R. pipiens*, as in other amphibians (40) (*D*). In GRGDS embryos, two distinct notochords appear at lateral positions (*E* and *F*). 4d monoclonal antibody, raised against chicken NCAM 180 kDa (36, 37), strongly stains the central nervous system (CNS) of control embryos (*G*). NCAM staining was detected as early as stage 18 (*H*) in GRGDS embryos along both sides of the embryo and intensified at stage 20 (*I*). *B*, *C*, *E*, *F*, and *H* are dorsal views, *I* is ventral, anterior is up in all cases. (*J*) Lateral view of a GRGDS embryo stained with LINC antibody (38) (anterior to the right) shows very similar pattern to NCAM staining (*H* and *I*). (*K*) This ventral view of a GRGDS embryo doubly stained with LINC (brown) and 12/101 (blue) shows that segmented somites are associated with LINC-positive tubular structures; anterior is up. (*L*) GRGDS embryo doubly stained with Tor 70 (brown) and 4d-NCAM (blue) antibodies; anterior is to the left. NCAM-positive cells are localized in the vicinity of each notochord while the midline of the ectoderm is unstained; note the apparent segmented spinal nerves. (*A–I*, bar = 1 mm; *J–L*, bar = 1 mm.)

embryos, or are other cells recruited under these conditions? To answer this question, fluorescent lineage tracers were injected into individual blastomeres of 32-cell stage embryos, and some of the embryos were injected with GRGDS peptide at stage 9. After embedding and sectioning at stage 21, the contribution of the progeny of labeled blastomeres to the notochord and the CNS was determined (Fig. 3). In intact embryos, the notochord is formed only by progeny of B1 (n = 8) and C1 (n = 11) blastomeres (Fig. 4*A*). The two notochords of GRGDS embryos likewise arise from B1 (n = 6) and C1 (n = 17) blastomeres (Fig. 4*B*). Thus, the cellular origin of the two ectopic notochords of GRGDS embryos is the same as that of the notochord of normal embryos (Fig. 3).

As summarized in Fig. 3, cells derived from the dorsal and lateral blastomeres of the A (n = 12) and B (n = 18) tiers (namely, blastomeres A1, A2, A3, B1, B2, and B3) populate the CNS of normal embryos, with the largest contribution coming from A1 and B1 (Fig. 4 *A* and *C*). Progeny of C tier blastomeres are very rarely found in the CNS of normal embryos. As will be presented elsewhere in detail, A tier blastomeres also contribute to the epidermis (Fig. 4*C*), B tier blastomeres contribute to somites, epidermis, and head mesenchyme (Fig. 4*F*), and C tier blastomeres contribute to somites, head mesenchyme, lateral plate, and prospective gut (Fig. 4*F*). In GRGDS embryos, the origin of putative neural cells has undergone a shift in a vegetal and ventral direction, although a large fraction of neural tissue derives from the B tier in GRGDS (n = 20) as in normal embryos. In GRGDS embryos, the progeny of A tier blastomeres (A1 and A3; n = 14) does not contribute to the ectopic nervous systems, these cells having exchanged their neural fate for an almost exclusively epidermal fate (Fig. 4 *D* and *E*). However, C tier blastomeres contribute substantially to neural tissue in these embryos (n = 26) (Fig. 4 *G–I*), in contrast to the almost complete absence of their contribution in the controls (n = 20). Further, while the CNS derives predominantly from dorsal (A1, B1) blastomeres in the control, neural cells in GRGDS embryos derive more evenly from dorsal and lateral

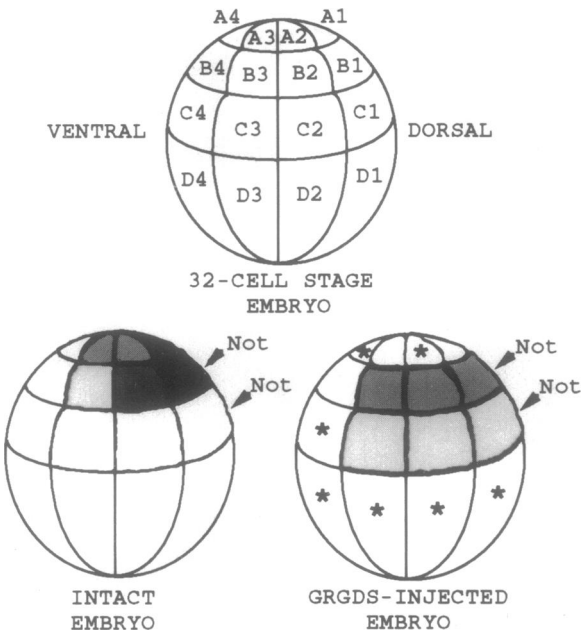

FIG. 3. Schematic representation of 32-cell stage blastomeres (*Upper*) and their contribution to notochord and CNS in normal (*Lower Left*) and GRGDS-injected (*Lower Right*) embryos. The notochord (arrowheads, Not) arise from blastomeres B1 and C1 in both normal and GRGDS embryos. Shading is proportionate to the contribution of each blastomere to the CNS; whereas the CNS originates from A and B tier blastomeres in control embryos, it originates exclusively from B and C tier blastomeres in GRGDS embryos. Asterisks indicate blastomeres whose fate was not determined.

cells (B1, B2, B3 and C1, C2, C3). Thus, inhibition of mesoderm involution leads to the following consequences. Axial mesoderm shows normal lineage derivation, but ends up in an abnormal lateral position; neural tissue forms in close apposition to the axial mesoderm from cells that have a more lateral–vegetal derivation than in the normal embryo.

DISCUSSION

The GRGDS Embryo as a Tool for the Study of Neural Induction. We have addressed the question of the general topology of neural induction in the amphibian embryo, especially the relationship between planar and vertical induction, by studying *R. pipiens* embryos with perturbed mesoderm involution. In agreement with earlier work (29) we find that injection of GRGDS peptide into the blastocoel of *R. pipiens* embryos prevents migration of the dorsal mesoderm across the blastocoel roof. Such embryos are a suitable object for studying the consequences of interrupting normal mesoderm–ectoderm contacts on neural induction and, potentially, other events. While the inhibition of mesoderm involution constitutes a major insult on development, it may be argued that GRGDS peptide is a rather specific inhibitor, for which there is good reason to believe that its only effect is interference with the binding of fibronectin to its receptor (45). Otherwise, the embryo remains whole, and the gross arrangement of germ layers—mesoderm underlaid by endoderm and surrounded by ectoderm—is maintained.

The GRGDS embryo may be contrasted with other preparations that are useful for studying neural induction. In the exogastrula, mesoderm moves away from the ectoderm, distorting shape and topology at least as much as in the GRGDS embryo. While exogastrulae and GRGDS embryos are superficially similar in that mesoderm involution is affected, the developmental outcomes are totally different: neural differentiation occurs at some distance from the final position of the notochord in the exogastrula (13), but notochord and neural differentiation are tightly linked in GRGDS embryos. The Keller sandwich, while being particularly well suited for detailed observation, involves apposing two ectoderm-marginal zone explants in a cell-type association not normally found in

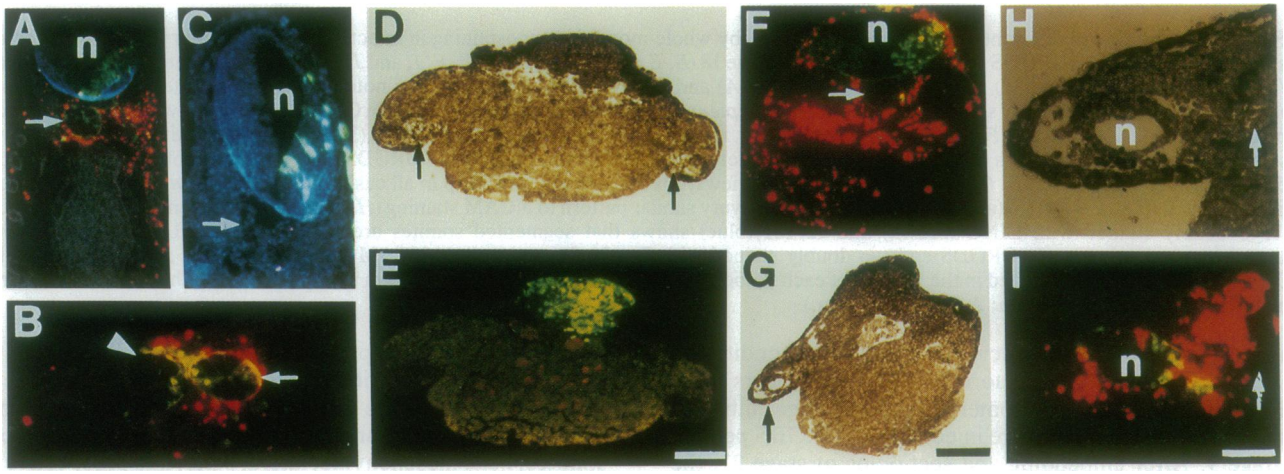

FIG. 4. Examples of lineage tracing of 32-cell stage blastomeres in control (*A*, *C*, and *F*) and GRGDS-injected embryos (*B*, *D*, *E*, *G*, *H*, and *I*), sectioned at stage 21. (*A* and *B*) B1 and C1 blastomeres were injected with FLDX (green) and TRLDX (red), respectively. Transverse section of a control embryo (*A*) shows B1 progeny in the spinal cord (n) and notochord (arrow); in this section C1 progeny does not appear in the notochord but in somites and mesenchyme. The notochord (arrow) of GRGDS embryo (*B*) contains B1- and C1-derived cells, and neural tissue (arrowhead) contains B1-derived cells. Blue staining in the ventolateral aspects of the neural tube (*A*; also in *C*) corresponds to immunostaining with a mix of 4d-NCAM and LINC antibodies visualized with AMCA fluorochrome. (*C–E*) Both A1 blastomeres were injected with FLDX. Transverse section of normal embryo (*C*) shows A1 progeny in the spinal cord (n) and the epidermis, while in the GRGDS embryo (*D*, phase-contrast; *E*, fluorescence), A1 progeny is restricted to the apical epidermal region; no labeled cells can be detected in a lateral position where neural tissue is located (see *I* and Fig. 2 *H–J* and *L*). Arrows in *D* point to the dual notochords. (*F–I*) The progeny of B2 (FLDX) and C2 (TRLDX) blastomeres in a normal (*F*) and a GRGDS (*G–I*) embryo. (*F*) In this section, B2 progeny is almost exclusively restricted to one half of the rhombencephalon (n). C2-derived cells form the pharynx and mesenchyme but are virtually absent from the rhombencephalon (n) and the notochord (arrow). (*G*) Phase-contrast image of an oblique transverse section of a GRGDS embryo showing only one of the two axes (arrow). (*H* and *I*) Higher magnification of the axis indicated in *G*. The neural tube-like structure (n) is composed of cells originating from B2 (green) and C2 (red) blastomeres, while the notochord (arrows in *H* and *I*) is not labeled. (*D* and *E*, bar = 0.3 mm; *A*, *F*, and *G*, bar = 0.2 mm; *C*, *B*, *H*, and *I*, bar = 0.1 mm.)

the embryo (21–23). The different preparations may thus reveal distinct aspects of normal cellular interactions.

Two Axes Form Laterally in GRGDS Embryos. Whole-mount immunostaining of GRGDS embryos with a notochord-specific monoclonal antibody (Tor 70) revealed an unexpected feature in the presence of two independent notochords positioned bilaterally. Moreover, the use of two neural markers (4d-NCAM and LINC) showed that neural differentiation in these embryos occurred only in the vicinity of each notochord and never along the dorsal midline of the ectoderm.

By lineage tracing we were able to demonstrate that (*i*) the two notochords of GRGDS embryos have the same origin as the notochord of normal embryos. This observation, together with the lateral location of the two notochords, indicates that, rather than migrating "North" across the blastocoel roof, dorsal mesoderm migrates "East and West" in GRGDS embryos, probably at the junction between the blastocoel roof and the endoderm. (*ii*) In addition to a contribution from B tier blastomeres as in normal embryos, the ectopic neural tissue in GRGDS embryos arises by the recruitment of the progeny of C tier blastomeres. In contrast to the normal situation, no A tier blastomere progeny contributes to the ectopic neural tissue (Fig. 3). These observations indicate that the lateral movement of chordamesoderm results in the induction of ectodermal cells that normally generate epidermis toward a neural fate by vertical signaling, while the midline of the ectoderm that continues to have planar contact with the dorsal lip fails to form any neural tissue. We conclude that vertical signaling is the dominant form of neural induction in this preparation.

Conclusions. Our emphasis on the importance of vertical signaling in neural induction in *R. pipiens* does not question the conclusion that planar signals are involved in A–P patterning of the neural plate in *X. laevis* (11–17), but we suggest that the relative significance of the different modes of neural induction is not settled at present. Beyond the different strength and limitations of the different preparations used, this divergence of emphasis could reflect differences in the gastrulation movements in the two species of frogs, since dorsal mesoderm has been reported to be initially located in distinct cell layers of the marginal zone in different anurans (46–48). Moreover, since gastrulation is an extremely rapid process in *X. laevis* (about 4 hr), vertical and planar pathways could represent redundant mechanisms that the embryo has enlisted to assure the formation of a well-organized nervous system. Such "double assurance" may be less important in *R. pipiens* where gastrulation lasts approximately 24 hr. While the role of alternate pathways of neural induction may be different in different vertebrates, our results serve to reemphasize the traditionally recognized importance of vertical signals from the mesoderm to the overlying ectoderm in this process.

We thank S. A. Moody and K. E. Johnson for valuable suggestions and communication of results before publication, R. P. Elinson for providing frogs from his colony, R. M. Harland and P. D. Kushner for Tor 70 antibody, and our colleagues Marcia O'Connell, Peter Good, and Michael Rebagliati for comments on the manuscript.

1. Spemann, H. & Mangold, H. (1924) *Wilhelm Roux's Arch. Entwicklungsmech. Org.* **100,** 599–638.
2. Holtfreter, J. (1933) *Wilhelm Roux's Arch. Entwicklungsmech. Org.* **129,** 669–793.
3. Mangold, O. (1933) *Naturwissenschaften* **21,** 761–766.
4. Hamburger, V. K. (1988) *The Heritage of Experimental Embryology: Hans Spemann and the Organizer* (Oxford Univ. Press, New York).
5. Saxén, L. (1989) *Int. J. Dev. Biol.* **33,** 21–48.
6. Guthrie, S. (1991) *Trends NeuroSci.* **14,** 123–126.
7. Kintner, C. R. (1992) *Annu. Rev. Neurosci.* **15,** 251–284.
8. Gilbert, S. F. & Saxén, L. (1993) *Mech. Dev.* **41,** 73–89.
9. Doniach, T. (1993) *J. Neurobiol.* **24,** 1256–1275.
10. Ruiz i Altaba, A. (1993) *J. Neurobiol.* **24,** 1276–1304.
11. Kintner, C. R. & Melton, D. A. (1987) *Development* **99,** 311–325.
12. Ruiz i Altaba, A. (1990) *Development* **108,** 595–604.
13. Ruiz i Altaba, A. (1992) *Development* **116,** 67–80.
14. Dixon, J. E. & Kintner, C. R. (1989) *Development* **106,** 749–757.
15. Doniach, T., Phillips, C. R. & Gerhart, J. C. (1992) *Science* **257,** 542–545.
16. Papalopulu, N. & Kintner, C. R. (1993) *Development* **117,** 961–975.
17. Zimmerman, K., Shih, J., Bars, J., Collazo, A. & Anderson, D. J. (1993) *Development* **119,** 221–232.
18. Sharpe, C. R. & Gurdon, J. B. (1990) *Development* **109,** 765–774.
19. Dirksen, M. L. & Jamrich, M. (1992) *Gene Dev.* **6,** 599–608.
20. Ruiz i Altaba, A. & Jessell, T. M. (1992) *Development* **116,** 81–93.
21. Keller, R. E. & Danilchik, M. (1988) *Development* **103,** 193–209.
22. Keller, R. E., Shih, J. & Sater, A. K. (1992) *Dev. Dyn.* **193,** 199–217.
23. Keller, R. E., Shih, J., Sater, A. K. & Moreno, C. (1992) *Dev. Dyn.* **193,** 218–234.
24. Johnson, K. E., Nakatsuji, N. & Boucaut, J.-C. (1990) in *Cytoplasmic Organization Systems*, ed. Malacinsky, G. M. (McGraw-Hill, New York), pp. 349–373.
25. Boucaut, J.-C., Johnson, K. E., Darribère, T., Shi, D. L., Riou, J.-F., Boulekbache, H. & Delarue, M. (1990) *Int. J. Dev. Biol.* **34,** 139–147.
26. Shi, D. L., Darribère, T., Johnson, K. E. & Boucaut, J.-C. (1989) *Development* **105,** 351–364.
27. Boucaut, J.-C., Darribère, T., Boulekbache, H. & Thiery, J. P. (1984) *Nature (London)* **307,** 364–367.
28. Boucaut, J.-C., Darribère, T., Poole, T. J., Aoyama, H., Yamada, K. M. & Thiery, J. P. (1984) *J. Cell Biol.* **99,** 1822–1830.
29. Johnson, K. E., Darribère, T. & Boucaut, J.-C. (1993) *J. Exp. Zool.* **265,** 40–53.
30. Keller, R. E., Danilchik, M., Gimlich, R. & Shih, J. (1985) *J. Embryol. Exp. Morphol.* **89,** Suppl., 185–209.
31. Keller, R. E. & Jansa, S. (1992) *Dev. Dyn.* **195,** 162–176.
32. Schlichter, L. C. & Elinson, R. P. (1981) *Dev. Biol.* **83,** 33–41.
33. Elinson, R. P. & Pasceri, P. (1989) *Development* **106,** 511–518.
34. Peng, H. B. (1991) *Methods Cell Biol.* **36,** 657–662.
35. Shumway, W. (1940) *Anat. Rec.* **78,** 139–147.
36. Watanabe, M., Frelinger, A. L. & Rutishauser, U. (1986) *J. Cell Biol.* **103,** 1721–1727.
37. Frelinger, A. L. & Rutishauser, U. (1986) *J. Cell Biol.* **103,** 1729–1737.
38. Steen, P., Kalghatgi, L. & Constantine-Paton, M. (1989) *J. Comp. Neurol.* **289,** 467–480.
39. Kintner, C. R. & Brockes, J. (1984) *Nature (London)* **308,** 67–69.
40. Bolce, M. E., Hemmati-Brivanlou, H., Kushner, P. D. & Harland, R. M. (1992) *Development* **115,** 681–688.
41. Hemmati-Brivanlou, A. & Harland, R. M. (1989) *Development* **106,** 611–617.
42. Nakamura, O. & Kishiyama, K. (1971) *Proc. Jpn. Acad.* **47,** 407–412.
43. Mould, A. P., Komoriya, A., Yamada, K. M. & Humphries, M. J. (1991) *J. Biol. Chem.* **266,** 3579–3585.
44. Sive, H. L., Hattori, K. & Weintraub, H. (1989) *Cell* **58,** 171–180.
45. Yamada, K. M. (1991) *J. Biol. Chem.* **266,** 12809–12812.
46. Keller, R. E. (1975) *Dev. Biol.* **42,** 222–241.
47. Smith, J. C. & Malacinski, G. M. (1983) *Dev. Biol.* **98,** 250–254.
48. Purcell, S. M. & Keller, R. E. (1993) *Development* **117,** 307–317.
49. Taira, M., Otani, H., Jamrich, M. & Dawid, I. B. (1994) *Development*, in press.